

## ***In Situ* Mössbauer Analysis of Hyperfine Interactions near Fe(110) Surfaces and Interfaces**

J. Korecki<sup>(a)</sup> and U. Gradmann

*Physikalisches Institut, Technische Universität Clausthal, D-3392 Clausthal-Zellerfeld, Federal Republic of Germany*

(Received 8 August 1985)

Hyperfine interaction parameters near clean and Ag-covered Fe(110) surfaces could be measured for the first time, for the first and the second monolayer separately, by means of *in situ* conversion-electron Mössbauer spectroscopy of oligatomic Fe(110) films on W(110) with monolayer <sup>57</sup>Fe probes. Quadrupole splitting deviates strongly from zero in the topmost monolayer only, indicating the reduced symmetry; it can be used to measure first- to second-layer self-diffusion. Magnetic hyperfine fields provide information on magnetic order near the surface with monolayer resolution.

PACS numbers: 73.20.Cw, 75.30.Et, 76.80.+y

Mössbauer spectroscopy offers unique possibilities for the local analysis of structural, electronic, and magnetic properties near surfaces, near interfaces, and in thin films. The idea is simple: If it is possible to prepare a single-crystal Fe film with an atomically smooth surface consisting of the non-Mössbauer isotope <sup>56</sup>Fe, in which exactly one monolayer is replaced by the Mössbauer isotope <sup>57</sup>Fe, and if it is possible to take a Mössbauer spectrum from that monolayer, the result is a literally local analysis of the hyperfine interaction parameters. The magnetic hyperfine field  $B_{\text{hf}}$  then forms a local probe of magnetism, giving experimental access to surface magnetism problems of high actuality like surface enhancement of ground-state magnetic order,<sup>1</sup> thermally induced decrease of magnetization near surfaces and in thin films,<sup>2</sup> and Friedel oscillations of magnetization or hyperfine field.<sup>1</sup> In addition, the quadrupole splitting  $\epsilon$  and isomer shift  $S$  give local information on electric-field gradient and electron density at the nucleus. If it is possible to do the experiment in ultrahigh vacuum (UHV) and to change intentionally the state of the surface by reactions with gases or coating of it with solid materials, then the local structure of the phenomena given above can be studied as a function of the electronic state of the surface (interface). The timely interest in such experiments is increased by recent *ab initio* band calculations of magnetic hyperfine fields near Fe(100) surfaces.<sup>3</sup>

It is the aim of the present paper to show that this simple idea can be realized by use of modern techniques of molecular beam epitaxy in UHV, in combination with monolayer-probe *in situ* conversion-electron Mössbauer spectroscopy (CEMS). Experimental values for  $B_{\text{hf}}$ ,  $\epsilon$ , and  $S$  in the topmost two layers of a clean Fe(110) surface are given for the first time. They are compared with the same features for Ag-coated Fe(110) surfaces.

A pioneering approximation to this local Mössbauer analysis has been given previously by Tyson *et al.*<sup>4</sup> They used Fe(110) films on Ag(111) films, prepared at room temperature at pressures  $< 10^{-6}$  Pa and coat-

ed by Ag, with Mössbauer spectroscopy in air in the transmission mode. They found an enhancement of  $|B_{\text{hf}}|$  near the surface in the ground state, which they interpreted as a confirmation of a surface-enhanced magnetization as predicted for Fe(100) by Wang and Freeman.<sup>1</sup> This interpretation has to be refined in the light of recent theoretical work of Ohnishi, Weinert, and Freeman,<sup>3</sup> who showed that the ground-state local structure of magnetic moment and of  $B_{\text{hf}}$  can be quite different. In addition, Tyson *et al.*<sup>4</sup> found a thermally induced decrease of  $|B_{\text{hf}}|$  near the surface, which certainly represents a decrease of surface magnetization.

The work of Tyson *et al.*<sup>4</sup> suffers from some problems which characterize the difficulty of the experiment. As they could not perform *in situ* structural tests of the film structure, they relied on an early epitaxial study of Fe(110) on Ag(111),<sup>5</sup> which shows a rich manifold of structural defects for the preparation conditions given, similar to that used by Tyson *et al.*, leaving many structural questions open, the answer to which should form the basis of a straightforward analysis. Furthermore, the use of transmission-type Mössbauer spectroscopy imposed severe limits of sensitivity and forced them to use <sup>57</sup>Fe probes of several monolayers, abandoning the intrinsic local resolution of the method. Finally, the free surface was not accessible to their approach.

Our experiments were performed in an UHV system (base pressure  $< 3 \times 10^{-9}$  Pa), equipped with a four-grid LEED optics, a cylindrical-mirror analyzer for Auger-electron spectroscopy (AES), and crucibles for molecular-beam epitaxy of a few metals, including <sup>57</sup>Fe, <sup>56</sup>Fe, and Ag, at  $p < 10^{-8}$  Pa. Fe(110) films of  $\approx 20$  monolayers (ML) only were prepared on a W(110) crystal. Their surface was clean in the sense that no impurities could be detected by AES; the extreme difficulties to get bulk Fe surfaces are avoided by use of thin films; impurities are avoided by avoiding the volume from which they are supplied at bulk surfaces. Film thickness could be determined with a quartz crystal oscillator having an absolute accuracy of  $\pm 5\%$  and reproducibility of  $\pm 0.1$  ML.

To find the optimum mode of preparation, we started from previous work of Waller and Gradmann,<sup>6</sup> who established layer-by-layer epitaxy of Fe(110) on W(110), for  $T \approx 500$  K. Periodic lattice distortions, caused by the misfitting substrate, fade out at  $\approx 10$  ML. We used stacks of 21 ML, for which the Fe lattice is undistorted in the topmost ten layers.

The standard preparation started with a base layer of  $D_1$  ML of  $^{56}\text{Fe}$ , prepared at 570 K. From visual inspection of the sharp LEED spots the distance of monatomic steps was estimated to be  $\geq 200$  Å. For the following deposition of the probe layer of  $D_2$  ML of  $^{57}\text{Fe}$ , the temperature was decreased to 420 K, thus avoiding  $^{57}\text{Fe}$ - $^{56}\text{Fe}$  interlayer diffusion, as discussed below. Coating by  $D_3$  ML of  $^{56}\text{Fe}$  at 420 K resulted in a  $D_1$ - $D_2$ - $D_3$  sample for the free surface, or a  $D_1$ - $D_2$ - $D_3$ /Ag sample for Ag coating, which was done again at 420 K. For Mössbauer analysis, the probe is transferred in front of a small-area  $^{57}\text{Co}$ /Rh source, working in air, irradiating the sample by  $\gamma$  quanta from a mean distance of 15 mm through a Be window at a grazing angle of  $15^\circ$  in the  $[1\bar{1}0]$  azimuth. Mössbauer nuclear resonances in the  $^{57}\text{Fe}$  probe layer are detected by use of 7.3-keV  $K$ -conversion electrons. To reduce a broad nonresonant background (photoelectrons, Compton electrons, and Auger electrons) from W,  $^{56}\text{Fe}$ , and  $^{57}\text{Fe}$ , electrons are filtered in an electrostatic analyzer (spherical condenser, transmission  $\approx 7\%$ , resolution  $\approx 4\%$ ) set to 7.3 keV, and then detected by a Channeltron. This results in a resonant effect of 5% of the background in the Mössbauer spectrum of one monolayer of  $^{57}\text{Fe}$  placed in a film of twenty layers of  $^{56}\text{Fe}$ . By use of a 100-mCi source, the spectrum of such a film could be recorded during 15 h with a signal-to-noise ratio of  $\approx 20$ .

Examples of Mössbauer spectra are shown in Fig. 1 for samples 19-1-1/Ag, 20-1/Ag, and 20-1. For all three spectra, the ratio of sextet line intensities is nearly  $I_1:I_2:I_3:I_4:I_5:I_6 = 3:0.14:1:1:0.14:3$ , which corresponds to an angle of  $15^\circ$  between incident  $\gamma$  rays and the magnetization  $\mathbf{J}_s$ . As we irradiate in the  $[1\bar{1}0]$  azimuth, this means that  $\mathbf{J}_s$  lies in the film plane, as expected from shape anisotropy; it further means that  $\mathbf{J}_s$  is along  $[1\bar{1}0]$ , in contrast to the bulk easy axis  $[001]$ . This switching of  $\mathbf{J}_s$  is caused by an in-plane magnetic surface anisotropy, as will be discussed in detail elsewhere.<sup>7</sup> For calibration of  $B_{\text{hf}}$ , we used thick samples ( $d > 100$  Å), the hyperfine field of which was set to 33.0 T at 295 K; the linewidth (FWHM) in these films was  $0.33 \text{ mm} \cdot \text{s}^{-1}$ , representing the intrinsic linewidth of our instrument. It is increased in comparison with the natural one ( $0.19 \text{ mm} \cdot \text{s}^{-1}$ ) by the finite angular width of the  $\gamma$  beam and by the high  $^{57}\text{Co}$  density in the source. Linewidths were increased to  $0.45 \text{ mm} \cdot \text{s}^{-1}$ ,  $0.50 \text{ mm} \cdot \text{s}^{-1}$ , and  $0.65 \text{ mm} \cdot \text{s}^{-1}$  for the 19-1-1/Ag, the 20-1/Ag, and the 20-1 sample, respec-

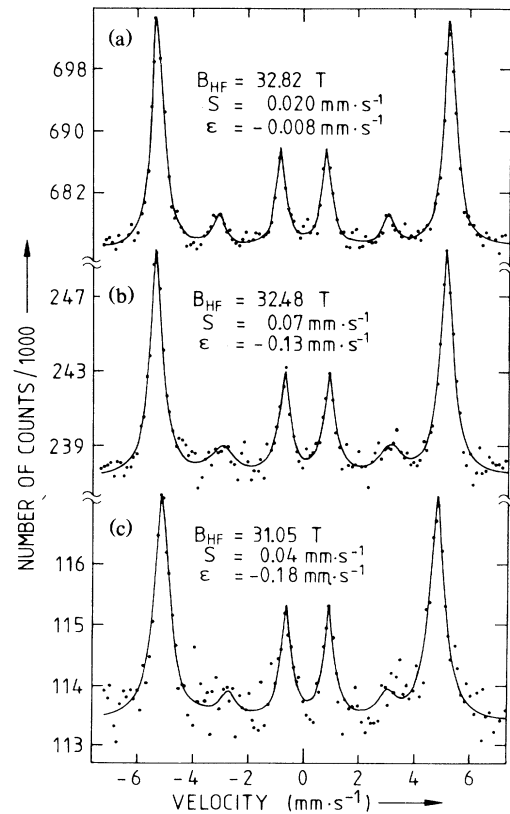


FIG. 1. Conversion-electron Mössbauer spectra of Fe(110) films on W(110), consisting of  $D_1$  ML of  $^{56}\text{Fe}$ , followed by  $D_2$  ML of  $^{57}\text{Fe}$  and eventually by  $D_3$  ML of  $^{56}\text{Fe}$ , called  $D_1$ - $D_2$ - $D_3$  with free,  $D_1$ - $D_2$ - $D_3$ /Ag with an Ag-coated surface. Spectra for (a) 19-1-1/Ag and (b) 20-1 Ag are taken in  $\sim 50$  and  $\sim 20$  h, respectively; for (c) the clean surface 20-1 in 8 h only. Hyperfine interaction parameters as given in the figures [ $\epsilon = (eQV_{zz}/8)(3 \cos^2\beta - 1)$ ].

tively. All lines remained symmetric.

A critical problem was the definite exclusion of  $^{56}\text{Fe}$ - $^{57}\text{Fe}$  interdiffusion, which forms the basis for our analysis. A first hint for the high-temperature limit to avoid this interdiffusion was taken from bulk and surface self-diffusion data<sup>8,9</sup> of Fe. We asked for a temperature for which  $[D(1000 \text{ s})]^{1/2}$  equals  $10^{-3}$  Å, resulting in 520 K for bulk and 420 K for surface self-diffusion, respectively. To confirm the reliability of 420 K as a diffusion-free temperature, we needed some property to be measured by CEMS, which is definitely different for a  $^{57}\text{Fe}$  ML probe in the first and in the second monolayer (counted from top of the film). This property is provided by  $\epsilon$ , which disappears in the bulk material by symmetry. For a 20-1/Ag preparation, however, we measured  $\epsilon = 0.128 \text{ mm} \cdot \text{s}^{-1}$  as a result of broken symmetry; to our knowledge, this forms the first measurement of  $\epsilon$  in an interface. Conversely, for the second ML, measured

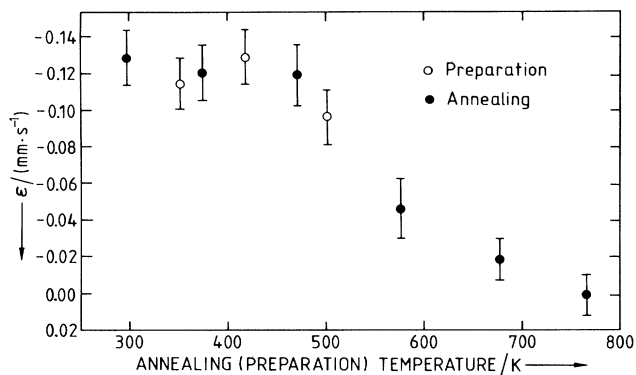


FIG. 2. Interdiffusion between the first and the second Fe ML in a 20-1/Ag sample, analyzed by a thermally induced change of the quadrupole splitting  $\epsilon$ . First, one series of samples (open circles) was prepared at preparation temperatures as indicated. Secondly, one sample, prepared at 420 K, was annealed at temperatures given (filled circles) for a period of about 40 h. Obviously, interdiffusion starts only above 450 K.

by 19-1-1/Ag,  $\epsilon$  disappeared ( $\epsilon = -0.008 \text{ mm} \cdot \text{s}^{-1}$ ), indicating the rapid screening of electrical fields in metals. For a further test for interdiffusion, we annealed the 20-1/Ag sample stepwise, as shown in Fig. 2. Only above 450 K did the decrease of  $\epsilon$  indicate interlayer diffusion. Finally, we prepared three 20-1/Ag samples at  $T_p = 350, 420,$  and  $500 \text{ K}$ . As shown in Fig. 2,  $\epsilon$  for  $T_p = 350 \text{ K}$  did not differ from that at  $T_p = 420 \text{ K}$ , again confirming that no interdiffusion takes place, which certainly should be enhanced at 420 K in comparison with 370 K. The surprisingly good agreement of our temperature limit with the estimate from bulk diffusion data indicates a good single-crystalline structure. Of course, some minor interlayer mixing caused by the growth process itself, at least for  $^{57}\text{Fe}$  probes lying deeper below the surface, must be considered.

One of the unique possibilities of our machine is the Mössbauer analysis of free surfaces. Immediately after preparation the Fe surfaces were atomically clean. However, residual gas adsorption could not be avoided because during one day the residual gas exposure was of the order of 1 L (1 Langmuir =  $10^{-6}$  Torr sec), the residual gas atmosphere consisting mainly of hydrogen with some water, methane, CO, and  $\text{CO}_2$  (as measured by a quadrupole mass spectrometer). If we assume an initial sticking coefficient  $S_0 = 0.16$  for hydrogen,<sup>10</sup> about  $\frac{1}{10}$  monolayer of hydrogen can be supposed one day after preparation. The same order of magnitude of C and O was detected by AES. To get data for the clean surface, we therefore measured spectra after preparation for a sequence of following periods, as shown in Fig. 3. We determined hyperfine parameters of the clean surface by extrapolation, as shown for  $|B_{\text{hf}}|$  in Fig. 3. To test reproducibility, two 20-1-type

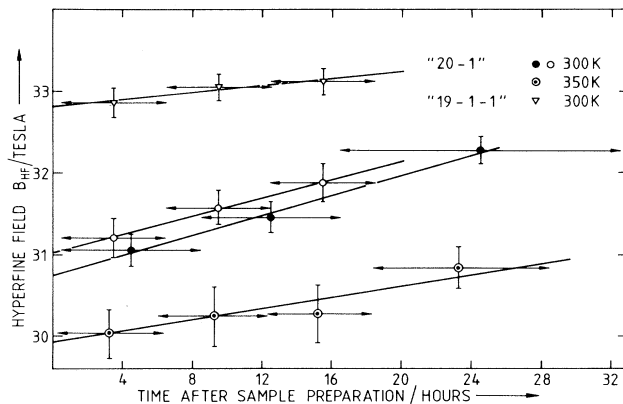


FIG. 3. Magnetic hyperfine field  $|B_{\text{hf}}|$  in the first and the second monolayers of uncoated Fe(110), taken from samples 19-1-1 and 20-1, respectively, shifting with time after preparation by residual gas adsorption. The temperature  $T$  of Mössbauer measurements is given in the figure.

preparations were measured at  $T = 300 \text{ K}$ ; the slight difference in  $|B_{\text{hf}}|$  may be connected with some minor admixture of second-monolayer atoms in one sample (open circles, 20-1.05; to be compared with filled circles), 20-0.96). The mean value is included in Table I below. One third 20-1 sample was measured at 350 K, to test for an alternative interpretation of the slowly shifting hyperfine fields in terms of some thermal relaxation of the film structure. The decrease of the slope of  $|B_{\text{hf}}|$  with increasing temperature indicates the decreasing sticking probability of residual gas molecules. In contrast relaxations should have been accelerated at the increased temperature and therefore can be excluded.

The results of our room-temperature measurements for the first and second atomic layers of the free and the Ag-covered Fe(110) surfaces are summarized in Table I. For comparison, the data in the center of the 21-monolayer film are included. Comparison with the results of Tyson *et al.*<sup>4</sup> can be only rough because they used probes of several monolayers. To perform this comparison, we use the difference

$$\Delta |B_{\text{hf}}| = |B_{\text{hf},i}| - |B_{\text{hf},\text{center}}|$$

between the hyperfine field in the  $i$ th monolayer and that in the center of the film. Within the limits of comparability and accuracy of measurements our results  $\Delta |B_{\text{hf}}| = -0.45 \text{ T}$  and  $-0.11 \text{ T}$ , respectively, for the first and the second monolayer agree with the value from Tyson *et al.*,  $\Delta |B_{\text{hf}}| = -0.46 \text{ T}$  for a probe consisting of nearly two surface layers. Tyson *et al.*<sup>4</sup> showed that this decrease is the result of an overcompensation of an enhancement in the ground state ( $\Delta |B_{\text{hf}}| = +0.78 \text{ T}$ ) by a thermally induced decrease ( $\Delta |B_{\text{hf}}| = -1.24 \text{ T}$ ). We certainly expect the same low-temperature surface enhancement for low-

TABLE I. Hyperfine interaction parameters (isomer shift  $S$ , quadrupole splitting  $\epsilon$ , and magnetic hyperfine field  $|B_{\text{hf}}|$ ) in the first and the second monolayer (counted from top) of 21 ML of Fe(110) on W(110), for both clean and Ag-coated surfaces, at 300 K. Data for clean surfaces from extrapolation like in Fig. 3; error for first layer includes deviation between two preparations in Fig. 3. For comparison, parameters are given for the central layer, too.

Surface	Layer	$S$ ( $\text{mm} \cdot \text{s}^{-1}$ )	$\epsilon$ ( $\text{mm} \cdot \text{s}^{-1}$ )	$ B_{\text{hf}} $ (T)
Fe clean	First	$+0.05 \pm 0.05$	$-0.18 \pm 0.04$	$30.88 \pm 0.40$
	Second	$-0.01 \pm 0.02$	$+0.035 \pm 0.020$	$32.80 \pm 0.15$
	Central	$-0.002 \pm 0.010$	$+0.006 \pm 0.010$	$32.91 \pm 0.07$
Ag/Fe	First	$+0.07 \pm 0.015$	$-0.13 \pm 0.015$	$32.48 \pm 0.08$
	Second	$+0.020 \pm 0.008$	$-0.008 \pm 0.008$	$32.83 \pm 0.06$
	Central	$+0.002 \pm 0.005$	$-0.001 \pm 0.006$	$32.93 \pm 0.05$

temperature measurements, which are in preparation.

The strong surface decrease of  $|B_{\text{hf}}|$  in the free surface ( $\Delta|B_{\text{hf}}| = -2.03$  T) can only in part be explained by thermal excitations, which can be estimated from the results of Tyson *et al.* Roughly 1 T can be estimated as a ground-state surface decrease of  $|B_{\text{hf}}|$ . This is in qualitative agreement with the much stronger decrease predicted for Fe(100) by Ohnishi, Weinert, and Freeman<sup>3</sup> ( $\Delta|B_{\text{hf}}| = -11.4$  T), as a result of atomic-like character of  $s$  electrons in the surface, which therefore give a positive contribution to  $B_{\text{hf}}$ , compensating in part the dominating negative contribution of core electrons. According to Ohnishi, Weinert, and Freeman, coating by Ag changes the character of  $s$  electrons, which now become itinerant and give a negative contribution resulting in  $\Delta|B_{\text{hf}}| = -2.4$  T only for the Ag-coated surface. This agrees qualitatively with our results for the Ag-covered films. The fact that the effects predicted by Ohnishi, Weinert, and Freeman for Fe(100) are so much stronger than our experimental results for Fe(110) may be connected with the more open character of the Fe(100) surface. Obviously, both experiments with Fe(100) and calculations for Fe(110) should be of great interest.

Our values of  $\epsilon$  were obtained with neglect of the deviation from rotational symmetry with respect to the surface normal. This approximation is justified both by the fact that we can fit the spectra using it and by an estimate of the asymmetry parameter  $\eta$  of the electric-field-gradient (EFG) tensor, resulting in  $\eta = 0.086$  only for the Fe(110) surface, in a point-charge model.  $\epsilon$  is then connected with the quadrupole moment  $Q$ , the angle  $\beta$  between  $B_{\text{hf}}$  and the EFG axis ( $z$  axis) and the EFG component  $V_{zz}$  by  $\epsilon = (eQV_{zz}/8)(\cos^2\beta - 1)$ . With  $Q = 0.216 \times 10^{-24}$   $\text{cm}^2$  and  $\beta = 90^\circ$ ,  $\epsilon$  from Table I results in  $V_{zz} = 32.9$   $\text{V} \text{ \AA}^{-2}$  and  $V_{zz} = 23.8$   $\text{V} \text{ \AA}^{-2}$  for the clean and the Ag-covered surfaces, respectively. To our knowledge,  $V_{zz}$  has been neither measured nor calculated previously.

The isomer shifts of our samples are in good agree-

ment with the results of Tyson *et al.*,<sup>4</sup> who measured  $S = 0.032 \pm 0.011$   $\text{mm} \cdot \text{s}^{-1}$  for a probe consisting of the topmost two layers. Within the limits of accuracy, this equals to the mean value of our first- and second-layer results. As discussed by Tyson *et al.*,<sup>4</sup> this positive  $S$  means a reasonable reduced density of  $s$  electrons, in agreement with calculations of Ohnishi, Weinert, and Freeman.<sup>3</sup>

We expect that the accuracy of the method is sufficient to detect Friedel oscillations of  $B_{\text{hf}}$  near the surface, if they exist, and their dependence on surface structure and temperature. Experiments are in preparation. As a whole we feel that monolayer-probe *in situ* CEMS forms a powerful new tool to analyze structural, electronic, and magnetic properties near surfaces.

This work was supported by the Stiftung Volkswagenwerk.

<sup>(a)</sup>Permanent address: Solid State Physics Department, Academy of Mining and Metallurgy, Krakow, Poland.

<sup>1</sup>C. S. Wang and A. J. Freeman, Phys. Rev. B **21**, 4585 (1980).

<sup>2</sup>U. Gradmann, G. Waller, R. Feder, and E. Tamura, J. Magn. Magn. Mater. **31-34**, 883 (1983).

<sup>3</sup>S. Ohnishi, M. Weinert, and A. J. Freeman, Phys. Rev. B **30**, 36 (1984).

<sup>4</sup>J. Tyson, A. H. Owens, J. C. Walker, and G. Bayreuther, J. Appl. Phys. **52**, 2487 (1981); J. Tyson, A. H. Owens, and J. C. Walker, J. Magn. Magn. Mater. **35**, 126 (1983); A. H. Owens, Ph.D. thesis, Johns Hopkins University, 1979 (unpublished).

<sup>5</sup>H. C. Snyman and G. H. Olsen, J. Appl. Phys. **44**, 888 (1973).

<sup>6</sup>G. Waller and U. Gradmann, Surf. Sci. **116**, 539 (1982).

<sup>7</sup>U. Gradmann, J. Korecki, and G. Waller, to be published.

<sup>8</sup>CRC Handbook of Chemistry and Physics, edited by R. C. Weast (CRC Press, Cleveland, 1977), 58th ed.

<sup>9</sup>Diffus. Defect Data **13**, 34 (1976).

<sup>10</sup>R. Imbuhl, R. J. Behm, K. Christmann, G. Ertl, and T. Matsushima, Surf. Sci. **117**, 257 (1982).